Inorganica Chimica Acta, 36 (1979) 275–279

An EPR Study of Copper(II) Ions in Tetrakis(salicylate)tetra-aquodicadmium(II). A Seven-coordinated Complex

R. DEBUYST, F. DEJEHET

Laboratoire de Chimie Inorganique et Nucléaire, 2, Chemin du Cyclotron, B-1348 Louvain-la-Neuve, Université de Louvain, Leuven, Belgium

C. GÖRLLER-WALRAND and L. G. VANQUICKENBORNE

Department of Chemistry, Celestijnenlaan 200F, B-3030 Heverlee, University of Leuven, Belgium

Received March 1, 1979

Cu(II) ions imbedded in the title-compound exhibit the following g and hyperfine values at 190 K: $g_1 = 2.432$, $g_2 = 2.100$, $g_3 = 2.076$, $A_1 = 1.056$ m^{-1}, $A_2 = 0.304$ m^{-1} *and* $A_3 = 0.242$ m^{-1}. *These EPR results can be reproduced within the framework of a ligand field model (*$\sigma \cong 0.6$ μm^{-1}, $\pi/\sigma \cong 0.2$, $\kappa = 0.4$ *and* $P = 2.4$ m^{-1}*) by assuming that a Cu(II) ion takes the place of a Cd(II) ion while preserving the pre-existing environment without major modifications.*

Introduction

A wealth of structural and theoretical information is available on first row transition metal ions coordinated by four or six ligands. Seven-coordinated complexes, although well known for the larger nd^N ions (n = 4 or 5) are much less common for first row transition metals. In recent years, however, a number of (usually polydentate) 3d^N complexes have been studied and the knowledge of their structure and properties is growing [1–3].

In the present note, we present the results of an EPR study of Cu(II) ions, imbedded in a tetrakis-salicylate Cd(II) matrix. Indeed, in this host crystal, the Cd(II) ion is surrounded by seven oxygen atoms in the first coordination sphere, forming a distorted pentagonal bipyramid. It seems reasonable to assume that a co-crystallized Cu(II) ion should be able to take the place of a Cd(II) ion, while preserving the pre-existing environment without major modifications.

Preparation of the Single Crystals

The synthesis is based on the difference in solubility of the salicylates of sodium, cadmium and copper. Doped single crystals are obtained by evaporating a saturated solution of cadmium salicylate, containing an appropriate concentration of Cu(II) ions. In the solutions, the Cu/Cd molar ratio was varied between 0.5 and 20%. The most suitable crystals for the EPR studies were obtained from a 10.9% solution, by dissolving the following quantities in one liter of water: 13.500 g (0.053 mol) of $3CdSO_4 \cdot 8H_2O$, 1.460 g (0.0058 mol) of $CuSO_4 \cdot 5H_2O$ and 18.726 g (0.117 mol) of sodium salicylate. It was not possible to obtain crystals with a higher copper content: increasing the Cu(II) concentration in the solution above 10.9% had no further effect on the crystal composition.

The crystal morphology is shown in Fig. 1a. While the undoped crystals are nearly colourless, the presence of Cu(II) ions gives them a uniform light-brown colour. Unfortunately, the absorption intensity was not sufficient to allow the registration of an

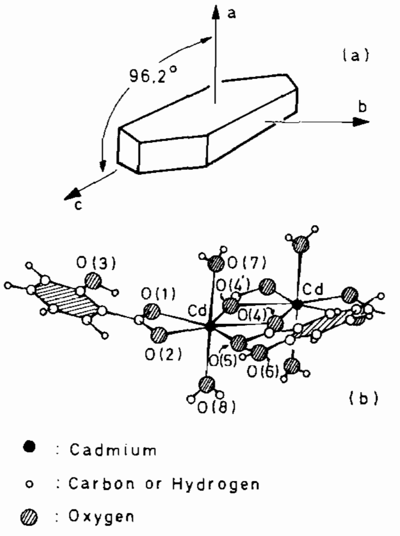

Fig. 1. (a) Crystal morphology and crystallographic axes. (b) Molecular structure of one dimer.

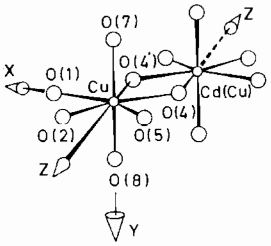

Fig. 2. Schematic representation of a paramagnetic center and the corresponding molecular coordinate system as suggested from the EPR-results.

optical spectrum. The position of the crystallographic axes was determined by means of X-ray rotation and Weissenberg photographs.

Crystallographic Data

The crystals of $C_{28}H_{28}Cd_2O_{16}$ are monoclinic [4] (space group $P2_1/c$) with a = 1.574, b = 1.247, c = 0.777 nm, β = 96.2° and Z = 2. They are obtained as tablets, elongated along the c-axis, characterized by well-developed faces in the (b, c) planes (Fig. 1a).

The unit cell contains two dimers, which are slightly inclined with respect to each other. Each dimer consists of two cadmium ions and four salicylate ligands, two of which are bridging; the salicylate ligands are bidentate through their carboxylic oxygen atoms. Figure 1b displays the molecular structure, using the atom numbering of reference [4]. Each Cadmium ion is surrounded by five oxygen atoms from the salicylate ions and by two other oxygen atoms from water molecules: O(7) and O(8). As shown in Fig. 1b, O(4) and O(4') are shared by the two Cd(II) ions, giving rise to a dimer structure which is centrosymmetric with respect to the midpoint of the O(4)–O(4') line. Fig. 2 shows a schematic representation of this situation and the coordinate system, as suggested from the EPR results.

The bond lengths and bond angles are collected in Table I. The five salicylate oxygen atoms coordinated to one given Cd ion are approximately coplanar (the sum of the five intra-salicylate O–Cd–O angles equals 359.3°). The two water–Cd bonds are approximately perpendicular to the plane of these five carboxylic oxygen atoms.

TABLE I. Bond Angles and Bond Distances [4] in Single Crystals of $C_{28}H_{28}Cd_2O_{16}$.

Bond Distances (in nm)	
Cd–O(1)	0.2325
Cd–O(2)	0.2438
Cd–O(5)	0.2314
Cd–O(4)	0.2530
Cd–O(4')	0.2291
Cd–O(7)	0.2321
Cd–O(8)	0.2246
Average Cd–O	0.2352
Intra-salicylate O–Cd–O Bond Angles	
O(1)–Cd–O(2)	54.7°
O(2)–Cd–O(5)	81.9°
O(5)–Cd–O(4)	52.9°
O(4)–Cd–O(4')	75.4°
O(4')–Cd–O(1)	94.4°
Average angle	71.9°
O(Water)–Cd–O(Salicylate) Angles	
O(7)–Cd–O(1)	86.2°
O(7)–Cd–O(2)	91.6°
O(7)–Cd–O(5)	88.4°
O(7)–Cd–O(4)	80.2°
O(7)–Cd–O(4')	83.6°
O(8)–Cd–O(1)	93.9°
O(8)–Cd–O(2)	96.6°
O(8)–Cd–O(5)	98.5°
O(8)–Cd–O(4)	98.0°
O(8)–Cd–O(4')	86.3°
Average angle	90.3°

Although the average O–Cd–O angle in the molecular XZ-plane is very close to 72°, the actual pentagon is far from regular (Table I); this point will be discussed in the next Sections.

The molecular Z-axes of one given dimer (Fig. 2) contain the two parallel Cd_I–O(4') and Cd_{II}–O(4) bonds. However, the Z-axes of the two dimers belonging to the same unit cell are not quite parallel: they form a small angle (of opposite sign) with the crystallographic b-axis. Similarly, the O(7)–Cd–O(8) direc-

TABLE II. Eigenvalues, g and A, and Eigenvectors (Direction Cosines of the Principal Axes) of the $\overline{\overline{g}}$ and $\overline{\overline{A}}$ Tensors in the a^*, b, c Reference Frame (T = 190 K). The estimated error is 0.001 on g_1, and 0.003 on g_2 and g_3; it amounts to 1 gauss on A_1 and 3 gauss on A_2 and A_3. The double signs refer to the two distinct paramagnetic centers.

g_1 = 2.432	A_1 = 1.056 m^{-1} (93 gauss)	g_1, A_1 : ±0.041	0.998	−0.048
g_2 = 2.100	A_2 = 0.304 m^{-1} (31 gauss)	g_2, A_2 : 0.999	∓0.039	±0.035
g_3 = 2.076	A_3 = 0.242 m^{-1} (25 gauss)	g_3, A_3 : ∓0.033	0.049	0.998

tions (molecular Y-axes) of the two dimers in the same cell form a small angle (again of opposite sign) with the crystallographic *c*-axis.

EPR Measurements

Single crystal EPR spectra were recorded at different temperatures (~150 K, ~190 K and 295 K), using an X-band Bruker spectrometer as previously described [5]. The crystals were analyzed in three orthogonal planes, two of which, (*c*, *b*) and (*c*, *a**) are crystallographic planes. The linewidth is temperature dependent (~6 gauss at 150 K, ~8 gauss at 190 K and ~22 gauss at ambient temperature). Two distinct paramagnetic centers are observed, with a slightly different orientation. The variation of the center of the two spectra and of the hyperfine splitting (^{63}Cu) has been measured in the (*a**, *b*) and the (*b*, *c*) planes. In the (*b*, *c*) plane, the two spectra are almost entirely superposed. The (*a**, *c*) plane was merely used to establish that the off-diagonal elements $(g^2)_{a^*c}$ and $(g^2A^2)_{a^*c}$ have to be zero; indeed, the (*a**, *c*) plane practically coincides with the molecular (X, Y) planes, as defined in Fig. 2, and a number of forbidden lines complicate the spectrum. The other matrix elements are obtained from the ($\underline{a}^*$, *b*) and (*b*, *c*) planes. Diagonalization of the $\bar{\bar{g}}$ and $\bar{\bar{A}}$ tensors [6] yields the eigenvalues and eigenvectors of Table II. The results of the Table refer to the data at T ~ 190 K, because the experimental conditions (crystal alignment, *etc.*) were optimal at that temperature.

The eigenvectors of the $\bar{\bar{g}}$ and $\bar{\bar{A}}$ tensors coincide within the limits of experimental error (*i.e* ~5°) and specify two different sites which are slightly inclined with respect to each other. Within the limits of precision of the method, the directions obtained for g_1, g_2 and g_3 coincide with the molecular directions, chosen as the Z, X and Y axes of Fig. 2. The eigenvalues for the two centers are identical and given by $g_1 \doteq 2.432$, $g_\perp = \frac{1}{2}(g_2 + g_3) = 2.088$, $A_1 = A_z = 93$ gauss and $A_\perp = 28$ gauss. It may be noted that g_z and A_z both decrease with increasing temperature (~0.3% for g_z, ~20% for A_z per 100 K), while $g_\perp$ and $A_\perp$ both increase with increasing temperature (~0.1% for $g_\perp$ and ~20% for $A_\perp$ per 100 K).

Discussion and Ligand Field Analysis

The experimental data can be understood by assuming that the doped crystals essentially preserve their structure except for the simple substitution of one Cd ion by one Cu ion, giving rise to a certain number of mixed Cd–Cu dimers.

Indeed, since every dimer is characterized by inversion symmetry, it makes no difference which one of the two Cd ions within a given dimer is replaced by Cu. As the unit cell contains two dimers (Z = 2) with different orientation, the observation of two, and only two, non-equivalent paramagnetic centers confirms the hypothesis.

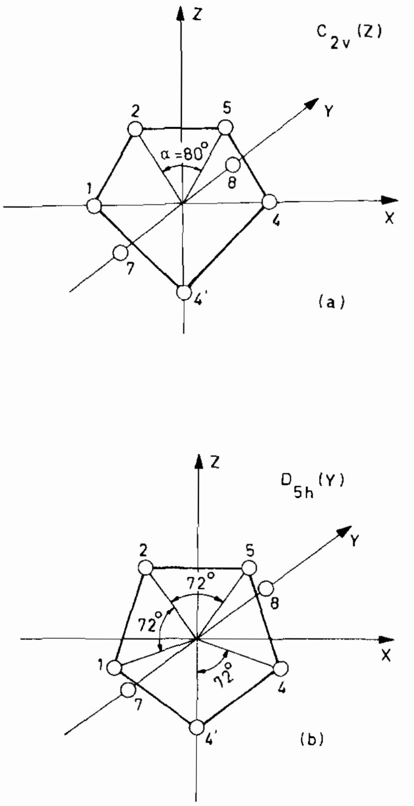

Fig. 3. Hypothetical and idealized structure of the paramagnetic center, where Cu(II) ion is at the origin. (a) C_{2v} structure where C_2 // Z. (b) D_{5h} where C_5 // Y-axis.

Strong additional support is provided by the relative orientation of the two g_z (g_1) eigenvectors, situated very nearly along the Cd–O(4′) direction. The angle between g_z and the XY-normal amounts to 1.6° for one center and 4.6° for the other. The g_2 direction is close to Cd–O(1) (X-axis), and g_3 to Cd(Cu)–O(8) (Y-axis).

Table I shows clearly that the actual symmetry is certainly not D_{5h}; it is much closer to C_{2v}, where the C_2 axis is situated along the Cd_I–O(4′) bond direction (g_1 or g_z); it should also be noted that the Cd_I–O(4′) bond is the shorter of the two bonds between Cd_I and the bridging oxygen atoms.

It is possible to rationalize the experimental g and A factors by using a simple ligand field approach. To this end, we use an additive point ligand model [7–8], where two one-electron parameters σ and π are associated to a given metal–ligand interaction.

Ideally, the σ- and π- parameters should be derived from the optical absorption spectrum. Since the latter could not be recorded from the single crystals under consideration, the parameters should be varied within reasonable limits [9–11].

As a first approximation, one lets the seven Cu–O interactions be characterized by one single set of (σ, π) parameters, thereby neglecting the effect of the different bond lengths. As for the angular position of the ligands, a C_{2v} picture of the first coordination sphere of Cu is shown in Fig. 3a. This picture is based on an idealization of the results of Table I (see also Figs. 1 and 2). This C_{2v} structure with the Z-axis as the C_2 rotation axis, can be looked upon as an octahedral wedge, where the sixth ligand (at +Z) of an octahedron has been replaced by two ligands, separated by a wedge angle of 80°. In this model, the small deviations from the angles in Table I seem justified by the fact that the replacement of Cd by Cu will certainly induce small distortions of unknown magnitude. Moreover, subsequent calculations with the exact angular values of Table I hardly changed the results.

A computer program was used to calculate and to diagonalize exactly the matrix of the ligand field, spin–orbit and Zeeman operators. The value of the spin–orbit coupling constant $\lambda = -0.0828$ μm^{-1} was used throughout for the spin–orbit coupling constant of the Cu(II) ion. Values of $\sigma \cong 0.8$ μm^{-1} characterize the typical Cu(II) complexes with bond lengths may be expected to be in the neighbourhood lengths may be expected to be in the neighborhood of 2.35 Å (the average Cd–O distance in the host crystal) and smaller σ values (down to 0.6 or 0.5 μm^{-1}) can be anticipated. The oxygen atoms belonging to carboxyl groups can be expected to be characterized by non-negligible π-interactions: a value of $\pi/\sigma \sim 0.2$ seems reasonable [9].

Fig. 4 shows an example of the type of results one obtains by using this range of parameters. The g-factors are quite sensitive functions of the ligand field parameters. They increase monotonically with decreasing σ (for a constant π/σ); for a constant σ, decreasing π/σ induces a cross-over between g_x and g_y.

The requirement of having $g_x > g_y$ (in order to reproduce the experimental results), together with the requirement that g_z should be much larger than the other two components leads to an optimal agreement for $\sigma = 0.6$ μm^{-1} and $\pi/\sigma = 0.2$: $g_z = 2.418$, $g_x = 2.150$, $g_y = 2.114$, comparing rather favorably with the experimental values of 2.432, 2.100 and 2.076 respectively. One might attempt to reproduce the experiment even better by allowing for the difference between the seven coordinating ligands, instead of treating them as identical (*i.e.* by means of *one* set of σ, π parameters). It turns out that g factors are particularly unsensitive to this type of corrections. For instance, accounting for the fact that Cu–O(4′) is the shortest bond length in the XZ-plane by increasing the σ-parameters (up to 25%) for the O(4′) ligand has almost no effect on g_z; it merely increases slightly the difference between g_x and g_y. One might consider the fact that the two ligands on the Y-axis are not carboxyl, but water groups, and therefore assign them a lower π/σ value. In this case g_x and g_y are virtually unaffected, while g_z decreases slightly.

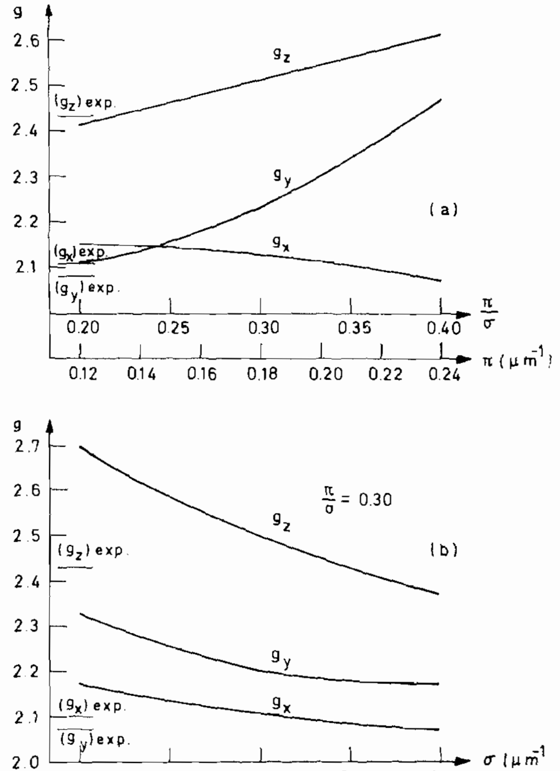

Fig. 4. Variation of the g-factors as a function of the ligand field parameters (a) σ fixed value (0.6 μm^{-1}) and variation of π/σ (b) π/σ fixed value (0.3) and variation of σ.

Therefore, an alternative fit (hardly better than the previous one) might be obtained by assigning ($\sigma = 0.53$ μm^{-1}, $\pi/\sigma = 0.2$) to the carboxyl oxygen atoms 1, 2, 4 and 5, ($\sigma = 0.66$ μm^{-1}, $\pi/\sigma = 0.2$) to the 'short' carboxyl–Cu bond (O = 4′) and ($\sigma = 0.53$ μm^{-1}, $\pi/\sigma = 0.1$) to the oxygen atom 7 and 8 (water ligands). Using these parameters, one obtains: $g_z = 2.425$, $g_x = 2.184$, $g_y = 2.098$, which is slightly worse for g_x, but slightly better for g_z and g_y than the previous result.

As for the angular variations of the ligands, two points should be stressed:

(i) if the wedge angle α is increased from $\alpha = 80°$ to $\alpha = 90°$, the g factors remain virtually unaffected;

(ii) if the wedge angle is decreased from $\alpha = 80°$ to $\alpha = 72°$, while at the same time displacing ligands 1 and 4 by 18° so as to generate a regular pentagon, one obtains a D_{5h} structure, with Y as the C_5 axis (Figs. 3b and 5). The two lowest a_1 orbitals are

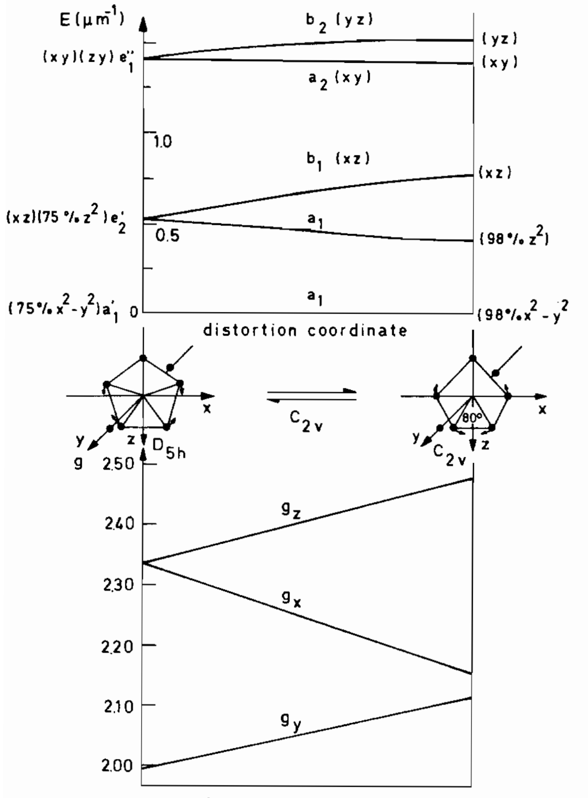

Fig. 5. Correlation diagram showing the angular distortion from a pentagonal bipyramid into an octahedral wedge (α = 80°). (a) energy levels (neglect of spin–orbit coupling) of the electron hole in Cu^{++}. (b) g-factors.

linear combinations of d_{z^2} and $d_{x^2-y^2}$, whose exact composition varies along the distortion coordinate as indicated in Fig. 5. The D_{5h} limit of these two orbitals follows from symmetry considerations: $a_1' = d_{y^2} = \sqrt{3}/2\ d_{x^2-y^2} + \frac{1}{2} d_{z^2}$, while $e_2'\,(a_1) = d_{x^2-z^2} = \sqrt{3}/2\ d_{z^2} - \frac{1}{2} d_{x^2-y^2}$. The distortion coordinate under consideration obviously has a very pronounced effect on the g factors, since now $g_z = g_x \gg g_y$ (Fig. 5). Clearly, one has good reasons to believe that the substitution of a Cd ion by a Cu ion takes place in an essentially undistorted site.

A final argument in favor of this hypothesis comes from the calculation of the hyperfine splitting pattern. In the standard expression of the hyperfine interaction operator [12, 14], one has to substitute the values of the parameters κ and P. Reasonable values for the Cu(II) ion [13, 14] are: κ from 0.2 to 0.4 and P from 2 to 4 m^{-1}. Carrying out the calculation on either of the two discussed crystal field parameter sets, one can calculate the A-tensor components as a function of κ and P. The tensor components are rather sensitive to variations in κ and P; a very reasonable fit could be obtained for κ = 0.4 and P = 2.4 m^{-1}. Both numbers fall within the range of acceptable values and yield A_z = 1.06, $A_x \sim 0.3$, $A_y \sim 0.25\ m^{-1}$, as compared to the experimental values of 1.056, ~0.304 and ~0.242 m^{-1} respectively.

Acknowledgments

E. Demelenne (Louvain, Belgium) is greatly acknowledged for his experimental contribution. Two of us (R.D., F.D.) are indebted to the Fonds National de la Recherche Scientifique (Belgium) for financial support.

References

1 R. A. Levenson and R. L. R. Towns, *Inorg. Chem., 13,* 105 (1974).
2 U. Rychlewska, R. C. Palenik, R. W. King and C. J. Palenik, *Chem. Comm.,* 799 (1975).
3 J. R. Wasson and D. R. Lorenz, *Inorg. Nucl. Chem. Letters, 11,* 617 (1975).
4 K. Venkatasubramanian, A. C. Villa, A. G. Manfredotti, and C. Guastini, *Cryst. Struct. Comm., 1,* 427 (1972).
5 R. Debuyst, D. Apers, and P. Capron, *J. Inorg. Nuclear Chem., 34,* 1541 (1972).
6 A. Lund and T. Vänngard, *J. Chem. Phys., 42,* 2979 (1965).
7 L. G. Vanquickenborne, C. Görller-Walrand, and R. Debuyst, *J. Magn. Resonance, 29,* 279 (1978).
8 L. G. Vanquickenborne, C. Görller-Walrand, and R. Debuyst, *J. Chem. Soc. Dalton,* 000 (1979).
9 L. G. Vanquickenborne and A. Ceulemans, *J. Am. Chem. Soc., 99,* 2208 (1977).
10 L. G. Vanquickenborne, J. Vranckx, and C. Görller-Walrand, *J. Am. Chem. Soc., 96,* 4121 (1974).
11 C. Görller-Walrand, J. Peeters, and L. G. Vanquickenborne, *J. Chim. Phys., 71,* 633 (1974).
12 F. Dejehet, R. Debuyst, B. Ledieu, J. P. Declercq, G. Germain and M. Van Meerssche, *Inorg. Chim. Acta, 30,* 197 (1978).
13 A. Abragam, J. Horrowitz, and M. M. L. Pryce, *Proc. Roy. Soc., A230,* 169 (1955).
14 F. E. Mabbs and W. R. Smail, *J. Chem. Soc. A,* 1716 (1970).